nature cell biology

The Diaphanous-related formin dDia2 is required for the formation and maintenance of filopodia

Antje Schirenbeck[1], Till Bretschneider[2], Rajesh Arasada[1], Michael Schleicher[1] and Jan Faix[1,3,4]

Formins have important roles in the nucleation of actin and the formation of linear actin filaments, but their role in filopodium formation has remained elusive. *Dictyostelium discoideum* Diaphanous-related formin dDia2 is enriched at the tips of filopodia and interacts with profilin II and Rac1. An FH1FH2 fragment of dDia2 nucleated actin polymerization and removed capping protein from capped filament ends. Genetic studies showed that dDia2 is important for cell migration as well as the formation, elongation and maintenance of filopodia. Here we provide evidence that dDia2 specifically controls filopodial dynamics by regulating actin turnover at the barbed ends of actin filaments.

Formins constitute a family of ubiquitous, highly conserved multi-domain proteins that are implicated in a wide range of actin-based processes such as cell polarization, cytokinesis and development[1–3]. These proteins are defined by a unique formin homology 2 (FH2) domain that is typically found in conjunction with an amino-terminally juxtaposed proline-rich FH1 domain[2]. Diaphanous-related formins (DRFs) are a subfamily marked by an additional FH3 domain that is required for subcellular localization[4], and two regulatory regions that allow regulation by Rho family GTPases[5]. Recently, the three-dimensional structures of the *Saccharomyces cerevisiae* formin Bni1p and the human formin Dia1 have been determined[6,7]. The crystal structure of the functional Bni1p FH2 dimer reveals a flexible tethered dimer architecture, consistent with a model in which the FH2 dimer walks as a processive cap at the barbed end during polymerization. The FH1 domain binds to profilin[8,9] as well as to SH3 and WW domain-containing proteins[10], and is believed to function as a scaffold that facilitates nucleation by recruitment of ATP–actin from profilin–actin complexes[11]. Except for the fission yeast cdc12p that requires FH1 and profilin together with FH2, the FH2 core domain and the intervening FH1FH2 linker region alone are necessary and sufficient to nucleate actin polymerization from G-actin *in vitro*[6,7,12].

In contrast to the Arp2/3 complex, which nucleates branched actin filaments, formins are implicated in the formation of linear actin filaments[3]. Linear actin filaments are prominent in yeast actin cables, stress fibres and filopodia. Although formin function could be clearly correlated with the establishment of actin cables and stress fibres[9,13], we are only beginning to understand the function of formins in filopodium formation[14,15]. Experimental measurements suggest that forces in the range of tens of piconewtons are required to allow growth of a filopodium against the resistance of the cell membrane[16]. Recently, formins have been identified to act as processive motors that can generate forces of at least 1.3 pN per actin filament[17,18]. Here we have analysed the role of *D. discoideum* Diaphanous-related formin dDia2. This protein is associated with the distal tips of filopodia and is required for the elongation of filopodial actin filaments.

The *D. discoideum* genome[19] (http://dictybase.org) indicates that this microorganism contains at least 10 different formin genes. In an attempt to characterize the DRFs within this group we screened the derived protein sequences for the presence of typical formin GTPase-binding domain (GBD) and Diaphanous autoregulatory domain (DAD) regulatory sequences[5]. We found that in addition to the previously described formins A and B[20], four other formins could be identified as *bona fide* DRFs. In this study, we characterize the *drf2* gene product dDia2. Sequence analysis of the *drf2* gene revealed the presence of three introns in the 5′ region, and therefore, the entire coding sequence of 3.25 kilobases (kb) was amplified from a cDNA library. The derived amino-acid sequence represents a polypeptide of 1,087 residues with an apparent relative molecular mass of 121,677. GDB and DAD regulatory sequences are located between residues 41–217 and 770–815, respectively, and the FH3 domain is positioned between residues 223–363. The proline-rich FH1 region is placed between residues 589–615, and FH2 is located between residues 633–1053. The schematic domain organization of this protein and an alignment of its GBD and DAD regulatory sequences with those of *Drosophila melanogaster* Diaphanous is depicted in Fig. 1a, b. dDia2 shows the highest overall degree of similarity with human dishevelled-associated-activator of morphogenesis hDAAM1 (30% identity; 42% similarity) and human hDia1 and hDia2 (~28% identity; 40% similarity).

The proline-rich FH1 domains are known to interact with profilin. In *D. discoideum* cells, profilin isoforms I and II are highly expressed[21], and profilin III is present only at low concentrations (unpublished observations). To determine the isoform specificity, we performed a yeast

[1]A. Butenandt-Institut/Zellbiologie, Ludwig-Maximilians-Universität, Schillerstr. 42, 80336 München, Germany. [2]AG Zelldynamik, Max-Planck-Institut für Biochemie, Am Klopferspitz 18a, 82152 Martinsried, Germany. [3]Present address: Institut für Biophysikalische Chemie, Medizinische Hochschule Hannover, 30623 Hannover, Germany.
[4]Correspondence should be addressed to J.F. (e-mail: faix@bpc.mh-hannover.de)

Published online: 22 May 2005; DOI: 10.1038/ncb1266

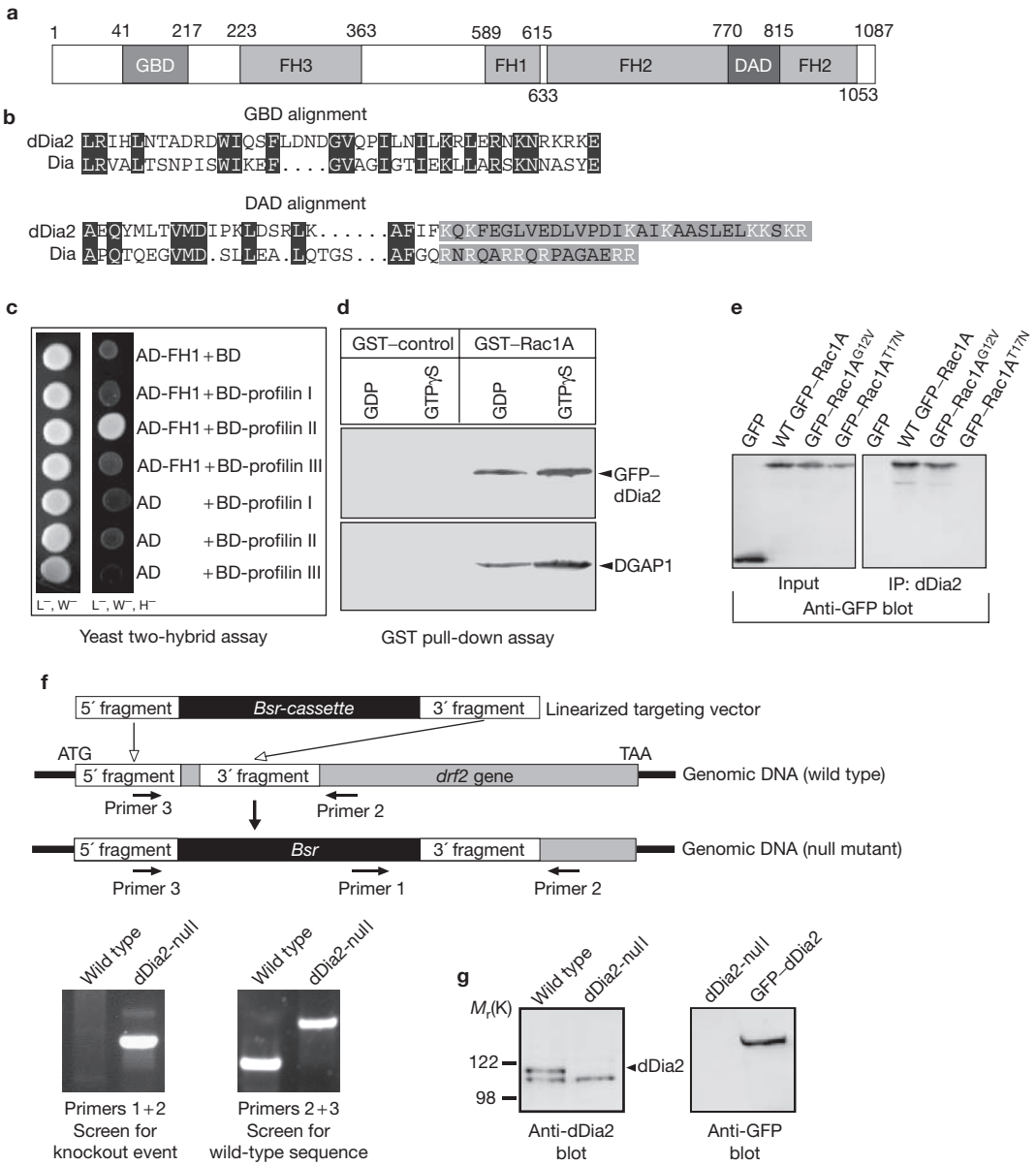

Figure 1 Domain organization of dDia2, interaction with regulatory proteins and generation of dDia2 mutants. (**a**) Schematic domain organization of dDia2. (**b**) Sequence alignment of GBD and DAD regions of dDia2 and *Drosophila* Diaphanous (Dia). Identical residues are shown as white letters on a black background. The basic region in DAD is shown in grey and basic residues are indicated as white letters. (**c**) The FH1 domain of dDia2 interacts specifically with the profilin II isoform in the yeast two-hybrid assay. Activation domain (AD), Gal4-activation domain; binding domain (BD), Gal4-binding domain. Yeast were transformed with the indicated constructs and tested for interaction by growth on selective media lacking leucine (L), tryptophane (W) or histidine (H). (**d**) GFP-tagged dDia2 interacts preferentially with the activated form of Rac1A. Cell lysates containing GFP-tagged dDia2 were incubated with beads containing the indicated GST constructs and then blotted for GFP monoclonal antibody 264-449-2. The Rac1A effector DGAP1 was used as a positive and GST as a negative control. (**e**) dDia2 interacts *in vivo* with Rac1A. dDia2 was immunoprecipitated from the cell lines indicated using dDia2-specific antibodies. The immunoprecipitates were subsequently analysed in immunoblots with anti-GFP monoclonal antibody 264-449-2. WT, wild type. (**f**) Inactivation of the *drf2* gene. Top shows the linearized *drf2* gene replacement construct that was used to replace the wild-type gene. dDia2-null mutants were identified by PCR using the specific primer pairs indicated. (**g**) Inactivation of the *drf2* gene was verified by western blotting using anti-dDia2 antibodies (left panel). Expression of GFP–dDia2 in dDia2-null cells was confirmed by western blotting using anti-GFP antibodies (right panel).

two-hybrid assay. This test clearly showed that dDia2-FH1 interacts specifically with profilin II (Fig. 1c). Other regulatory proteins that bind to, and apparently activate, DRFs are the Rho family GTPases Cdc42, Rho and Rac. Although no Cdc42 or Rho homologues are known in *D. discoideum*, cladistic analysis has identified 15 Rac proteins[22]. We therefore investigated whether dDia2 is capable of interacting with the three well characterized GTPases Rac1A, RacE and RacC, using glutathione *S*-transferase (GST) fusion constructs expressed in *Escherichia coli*. The glutathione Sepharose-bound GTPases were loaded with either GDP or GTP-γS, and incubated with lysates that had been prepared from a cell line expressing green fluorescent protein (GFP)-tagged dDia2 in dDia2-null cells (Fig. 1d, g). After repeated washing of the beads, the presence of bound GFP–dDia2 was analysed by western blotting with GFP-specific monoclonal antibody 264-449-2. As shown in Fig. 1d, dDia2 as well as the Rac1A effector DGAP1 as a control bound strongly to Rac1A, but not to GST alone. No binding of dDia2 was detected with RacE and

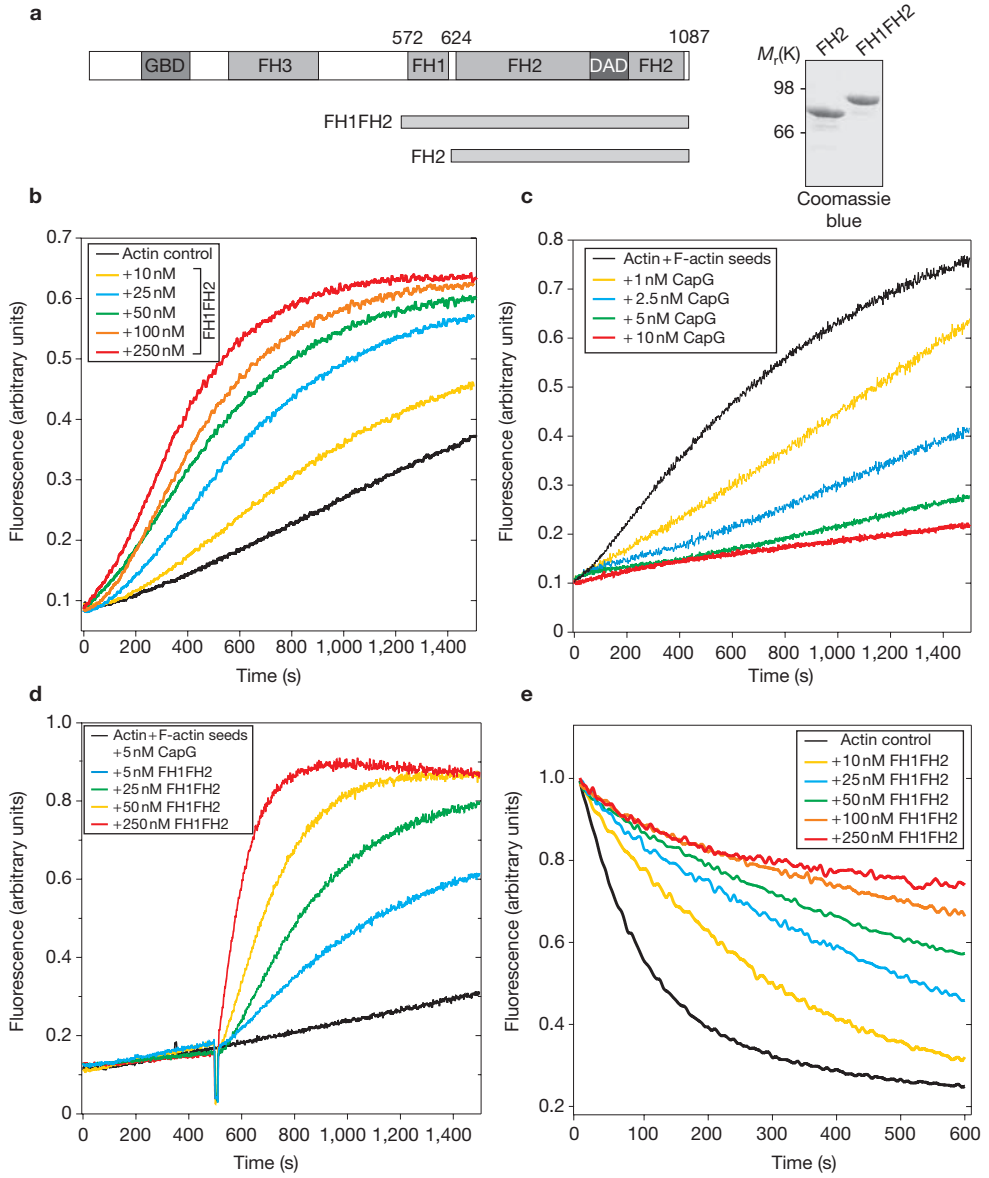

Figure 2 Interaction of the FH1FH2 construct with actin. (**a**) Left: schematic representation of the constructs used. Right: Coomassie-blue-stained SDS-polyacrylamide gel with purified FH2 and FH1FH2 polypeptides. (**b**) FH1FH2 promotes actin polymerization. Actin (1.2 μM; 8% pyrene-labelled) was polymerized in the presence of 0 nM (black; bottom) to 250 nM (red; top) FH1FH2. (**c**) Inhibition of actin polymerization by capping protein (CapG). Actin (1.4 μM; 10% pyrene-labelled) and F-actin seeds were polymerized in the presence of 0 nM (black; top) to 10 nM (red; bottom) CapG. (**d**) FH1FH2 removes capping protein from filament ends. Actin (1.4 μM; 10% pyrene-labelled) was polymerized in the presence of 5 nM capping protein, which strongly inhibited polymerization (black; bottom). After 500 s, increasing nanomolar concentrations of FH1FH2 were added. (**e**) FH1FH2 inhibits depolymerization of actin. F-actin (63% pyrene-labelled) was diluted below the critical concentration of the barbed ends (0.1 μM) in polymerization buffer alone or in polymerization buffer that contained increasing amounts of FH1FH2. Essentially the same results were observed with recombinant Cap32/34, the *D. discoideum* orthologue of CapZ (data not shown).

RacC (data not shown). The association of GFP–dDia2 with Rac1A was greater when GTP-γS was bound to the GTPase, indicating that dDia2 binds preferentially to the activated, GTP-bound form of Rac1A. To test whether Rac1A also interacts with dDia2 *in vivo*, dDia2 was immunoprecipitated with polyclonal dDia2-specific antibodies from cell lines expressing GFP or GFP-tagged wild-type, constitutively active (G12V), as well as dominant-negative (T17N) forms of Rac1A[23]. Analysis of the immunoprecipitated proteins by western blotting with GFP antibodies revealed that wild-type Rac1A and Rac1A^{G12V} were co-precipitated with dDia2 (Fig. 1e). Because wild-type Rac1A is able to cycle between GTP- and GDP-bound forms and no binding was seen with Rac1A^{T17N}, we conclude from these results that dDia2 interacts with the activated form of Rac1A *in vivo*. These findings are consistent with a previous study that revealed Rac1A to be part of a signalling pathway that is required for filopodium formation in *D. discoideum*[24]. Nevertheless, we cannot exclude the possibility that other Rac family members from *D. discoideum* are also involved in this pathway.

To test whether dDia2 nucleates actin polymerization *in vitro*, a large number of dDia2 expression constructs were made. Of these, only two were soluble and were expressed in adequate amounts as GST fusions

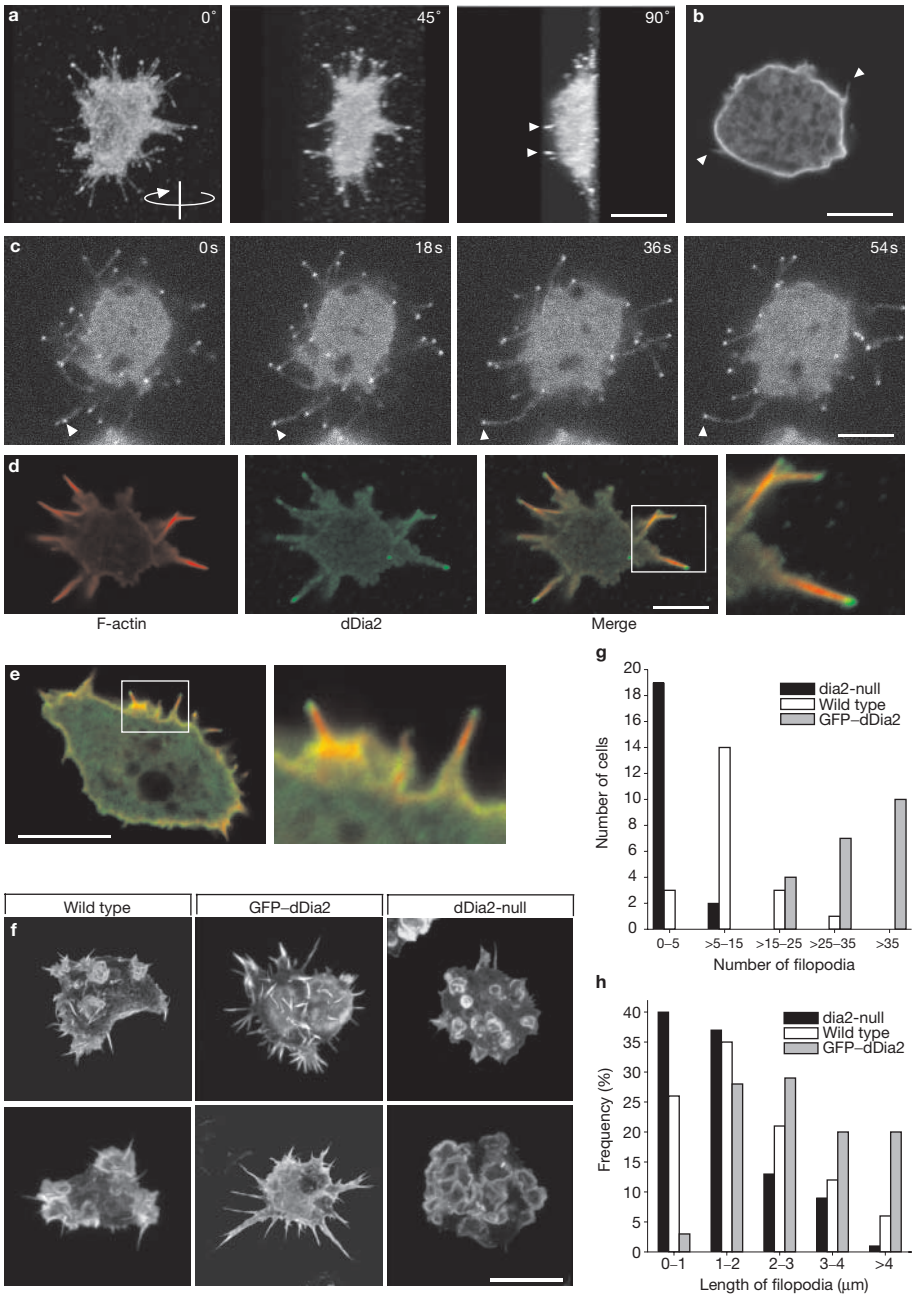

Figure 3 dDia2 localizes to filopodial tips and is required for the formation of filopodia. (**a**) Full-length dDia2 localizes to the tips of substrate-attached and free filopodia. The GFP–dDia2 cell shown was fixed and labelled with anti-GFP polyclonal antibodies. Starting at the bottom of the cell, confocal sections were taken in steps of 0.2 μm. Maximum projections for different viewing angles of the resulting image stack illustrate the accumulation of dDia2 in free (white arrowheads) and attached filopodia. (**b**) Confocal section through a wild-type cell expressing a C-terminally truncated form of dDia2 (residues 1–425) tagged with GFP. The cell was labelled with anti-GFP polyclonal antibodies. White arrowheads indicate filopodia. (**c**) GFP–dDia2 is concentrated at the tips of growing filopodia. A time-lapse series from a GFP–dDia2 cell at 18-s intervals in one confocal plane is shown. The tip of one growing filopodium is marked with a white arrowhead in each panel. (**d**) dDia2 accumulates at the ends of actin filaments. A GFP–dDia2 cell was labelled with TRITC–phalloidin to visualize F-actin (red), and anti-GFP antibodies to label GFP-tagged dDia2 (green). The merged image shows dDia2 accumulation at the globular filopodia tips at the ends of the actin bundles (boxed area is shown at a higher magnification on the far right). (**e**) Endogenous dDia2 at filopodia tips (boxed area is shown at a higher magnification on the right). A wild-type cell was labelled for dDia2 with anti-dDia2 polyclonal antibodies (green) and for F-actin with TRITC–phalloidin (red). (**f**) Cell morphology and F-actin organization in wild-type cells and dDia2 mutants. The cells were fixed and labelled with TRITC–phalloidin to visualize F-actin. Three-dimensional reconstructions were computed from confocal sections. Scale bars, 5 μm (**a**–**f**). (**g**) Quantification of filopodia numbers in wild-type cells and dDia2 mutants. (**h**) Quantification of filopodium length in wild-type cells and dDia2 mutants. Pairwise testing of the distributions showed that differences in filopodia numbers as well as lengths are highly significant ($P < 0.01$, Mann–Whitney U-test).

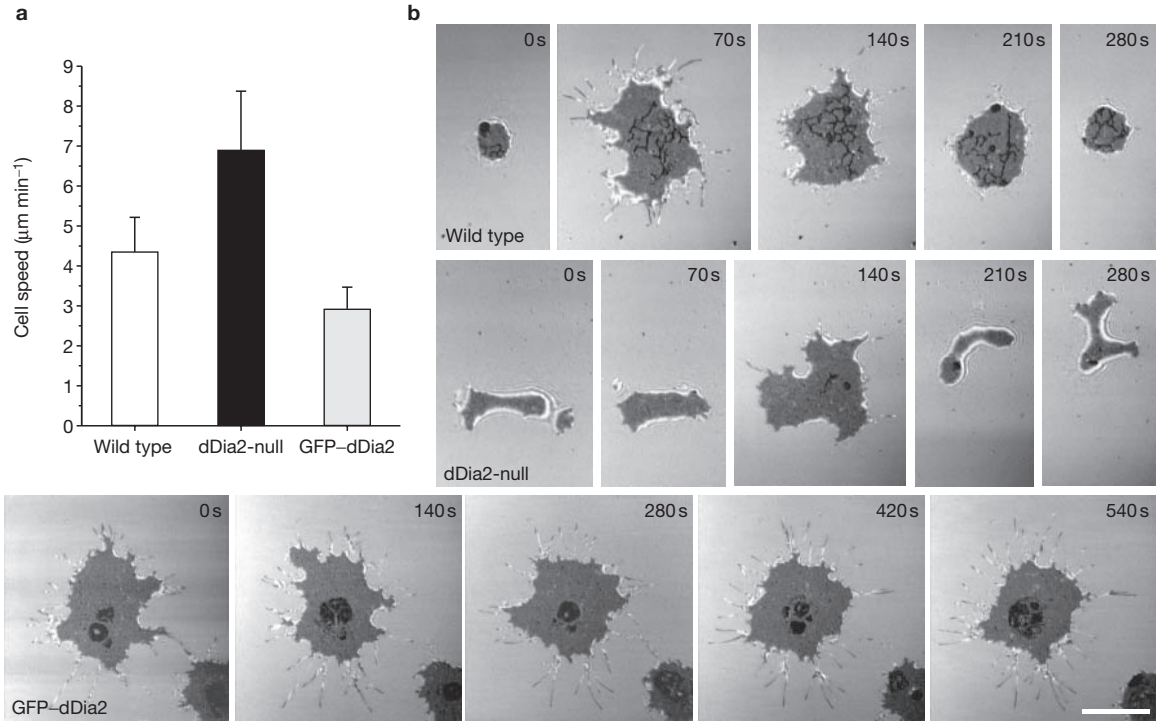

Figure 4 Motility and RICM analysis. (**a**) Quantification of cell motility for wild-type cells and dDia2 mutants in nutrient medium. The bars show the mean values for the cell velocities obtained from 70 cells from each cell line (error bars represent s.d.). The differences between these strains were highly significant ($P < 10^{-4}$; two-sided *t*-test). (**b**) RICM analysis of wild-type and dDia2 mutants. RICM micrographs of wild-type, dDia2-null and dDia2-overexpressing cells migrating on an uncoated glass surface during growth phase. The dark areas indicate where the cells are in close proximity to the substratum (<100 nm). The shown images are representative frames from time-lapse series (see Supplementary Information, Movies 3–5). The measured average contact areas for the whole series are 98.4.6 ± 58.8 μm^2 (± s.d.) for the wild-type cell, 56.0 ± 43.6 μm^2 for the dDia2-null mutant, and 162.4 ± 10.0 μm^2 for the GFP–dDia2-overexpressing cell. Please note the different timescale for the GFP–dDia2 cell. Scale bar, 10 μm.

in *E. coli* (Fig. 2a). One construct contained the FH2 domain and most of the N-terminal linker sequence (FH2: residues 624–1087), the other harboured the FH1 domain together with the connecting linker and the adjacent FH2 domain (FH1FH2: residues 572–1087). Purified FH2 alone did not show any interaction with actin (data not shown) perhaps because it did not contain the complete linker region connecting the FH1 and FH2 domains. The linker has been shown to be required for dimerization of the FH2 core domains[6,7]. Nanomolar concentrations of FH1FH2 significantly increased the rate of spontaneous actin polymerization (Fig. 2b). Although the FH1 domain of dDia2 was found to interact specifically with the profilin II isoform in the yeast two-hybrid assay, profilin *per se* was not required for the nucleation of actin *in vitro*. However, we cannot exclude that dDia2 requires profilin II to increase the processivity of actin assembly as it was described for the mouse formin mDia1 (ref. 17). To test the filament uncapping activity of dDia2, we first titrated the inhibition of filament elongation by adding increasing amounts of CapG/macrophage capping protein. As seen from Fig. 2c, 5 nM capping protein almost completely inhibited actin polymerization in 1.4 μM actin. Addition of FH1FH2 to capped actin filaments initiated a rapid onset of filament elongation (Fig. 2d). This suggested that FH1FH2 efficiently removed the capping protein and made the barbed filament ends accessible to actin monomers. This assumption was corroborated by F-actin depolymerization assays in the absence or presence of FH1FH2. Nanomolar concentrations of FH1FH2 efficiently inhibited the rate of actin depolymerization by blocking the barbed ends (Fig. 2e). Thus, dDia2 exerts the following typical formin properties: (1) it interacts with barbed ends (Fig. 2e); (2) it removes capping protein and, unlike a true capping protein, supports elongation of F-actin seeds at an extremely high rate (Fig. 2d); and (3) to a lesser extent it nucleates actin polymerization from scratch (Fig. 2b).

To investigate the specific functions of dDia2, we deleted the *drf2* gene and, in addition, expressed full-length GFP-tagged dDia2 in dDia2-null mutants (GFP–dDia2). GFP-labelled dDia2 showed a strong enrichment at the ends of substrate-attached and free filopodia, indicating that its localization is independent of cell–substratum contact (Fig. 3a). The subcellular distribution of endogenous dDia2, as visualized with polyclonal anti-dDia2 antibodies, was similar (Fig. 3e). Because the FH3 domains of other formins were previously shown to be responsible for the subcellular localization[4,20], we expressed a carboxy-terminally truncated dDia2 construct (residues 1–425) that lacked the FH1FH2 region. This construct no longer accumulated in filopodial tips but showed a strong enrichment in the entire cortical region, indicating that the elements from the FH1FH2 region contribute to targeting of dDia2 to filopodial tips (Fig. 3b). dDia2 constructs that lack the FH3 (Δ223–363) or only contain the predicted FH3 domain (223–363) were both diffusely distributed in the entire cytoplasm, but we cannot rule out that these constructs were misfolded (data not shown). We conclude that the N terminus of the protein (including the FH3 domain) targets the protein to the cell cortex and that FH1FH2 refines the localization specifically to filopodial tips. In preliminary experiments, profilin I/II-minus cells[21] that expressed

GFP–dDia2 generated shorter and fewer filopodia and, most interestingly did not accumulate dDia2 at filopodia tips (data not shown).

Four-dimensional confocal microscopy with these cells revealed that dDia2 remained bound to the tips of mature and growing filopodia (Fig. 3c, and see Supplementary Information, Movie 1). To determine how dDia2 is localized in these structures with regard to the actin system, GFP–dDia2 cells were fixed and double-labelled for dDia2 and F-actin. As shown in Fig. 3d, the region of strongest GFP–dDia2 enrichment was confined to a small region between the tips of filopodia and the ends of the actin filaments, consistent with the biochemical results, indicating that dDia2 regulates the barbed ends of actin filaments (for an animated three-dimensional reconstruction see Supplementary Information, Movie 2). An intensity profile of GFP–dDia2 accumulation showed a ~10-fold fluorescence increase in the tip regions. To evaluate the role of dDia2 in filopodium formation we compared the ability of wild-type amoebae and dDia2 mutants to form filopodia. In contrast to wild-type cells, dDia2-null mutants showed severe defects in filopodia number and morphology (Fig. 3f). Conversely, GFP–dDia2 cells generated more and considerably longer filopodia than wild-type cells, indicating a specific requirement for dDia2 in filopodia formation (Fig. 3g, h). The overexpression of GFP–dDia2 was approximately fivefold compared with wild-type cells (data not shown).

The strong label of filopodial tips in GFP–dDia2 cells allowed us to determine the dDia2-mediated filopodial growth rate. Using the cell shown in Supplementary Information, Movie 1, we tracked 14 filopodia and selected only the time frames in which the individual filopodia stayed in one focal plane without bending up- or downwards. The average growth rate was 2.16 ± 0.57 μm min^{-1} (± s.d.; $n = 20$), which is in good agreement with the average cell motility of 2–4.5 μm min^{-1} of *D. discoideum* wild-type cells during growth phase. This suggests that the elongation rate of actin filaments in filopodia or in lamelipodia at the moving front is comparable.

A quantitative analysis of filopodia numbers and lengths in wild-type and mutant cells was obtained from three-dimensional reconstructions that were computed from confocal image sections for 20 typical cells of each cell line (Fig. 3f). Most wild-type cells contained between 5 and 15 filopodia, whereas all analysed GFP–dDia2 cells had more than 15, some of them even up to 100 filopodia. In marked contrast, most dDia2-null cells developed fewer than five filopodia (Fig. 3g). In addition, this analysis revealed that filopodia are shorter in the null mutant and longer in GFP–dDia2 cells when compared with wild-type cells (Fig. 3h). In conclusion, these results provide a clear correlation between dDia2 expression and filopodium formation.

Filopodia are used by many cell types as sensing organs to explore environmental cues and they seem to be implicated in cell motility as well as in cell–substrate adhesion[25–28]. To examine whether dDia2 expression affects cell motility, random cell migration in nutrient medium was determined using a quantitative motility assay. The measured rates of cell migration were 4.3 ± 0.9 μm min^{-1} (± s.d.) for wild-type cells, 6.9 ± 1.5 μm min^{-1} for dDia2-null mutants, and 3.1 ± 0.5 μm min^{-1} for GFP–dDia2-overexpressing cells (Fig. 4a). These findings demonstrated an inverse correlation between dDia2 expression and cell motility, and revealed that filopodia are not essential for motility of *D. discoideum* amoebae during growth phase. In addition, we conclude from these data that an overexpression of the formin dDia2 does not necessarily increase motility, despite its assumed function of stimulating the elongation rate as a processive cap at barbed filament ends.

Because cell migration is also affected by cell-to-substratum adhesion, we used reflection interference contrast microscopy (RICM) to examine cell migration patterns on an uncoated glass surface as well as the dynamics of filopodia that emanate from the ventral surface of the cells. Wild-type cells continuously spread out and subsequent contractions reduce the contact area of the cell with the substratum. After attachment to the glass surface, filopodia extended and retracted in periods of less than 60 s (Fig. 4b, upper panels; see Supplementary Information, Movie 3). Wild-type cells and dDia2-null mutants showed similar patterns, although in the mutant the overall contact area was considerably reduced and occasionally a few cellular protrusions resembling unstable filopodia occurred (Fig. 4b, middle panels; see Supplementary Information, Movie 4). In marked contrast, the cells overexpressing dDia2 continuously showed a large contact area. Furthermore, numerous filopodia that were formed by these cells attached strongly to the glass and were stably maintained, sometimes for more than 20 min (Fig. 4b, lower panels; see Supplementary Information, Movie 5). Taken together, these findings demonstrate that the control of filopodial dynamics by dDia2 is implicated in the regulation of cell–substrate adhesion as well as cell motility.

Our data show that dDia2, a member of Diaphanous-related formins in *D. discoideum*, has all the characteristic properties of a formin *in vitro*. *In vivo* it is specifically involved in the formation and maintenance of filopodia. These results are consistent with the previous findings from Hug *et al.*[29], who investigated the role of *D. discoideum* capping protein Cap32/34 in the formation of filamentous actin structures. Overexpression of the capping protein reduced the number and the length of filopodia, whereas a knockdown in the protein level increased the number of free barbed ends, which consequently resulted in more filopodia. These results indicated that an uncapping step by a then unknown player is necessary for the formation and elongation of filopodia. Our data suggest that this unknown player could be the formin dDia2.

METHODS

Cell culture and transformation of *D. discoideum* cells. Cells of *D. discoideum* AX2 wild-type strain and of derived transformants were cultivated and transformed by electroporation as described[23]. Null mutants were screened by the polymerase chain reaction (PCR) using the PCR template purification kit (Roche, Penzberg, Germany).

cDNA cloning and generation of transformation vectors. For cloning and expression of GFP–dDia2, the entire coding region of the *drf2* gene was amplified from cDNA by PCR as a 3.25-kb *Bam*HI/*Sal*I fragment, cloned into pDGFP-MCS-Neo[30], and the sequence verified. The *drf2* sequence has been deposited in the EMBL database (accession number AJ748258). For expression of a C-terminally truncated form of dDia2 (residues 1–425) the corresponding region was amplified from *drf2* cDNA and cloned as described above. For construction of the *drf2* targeting vector, a 750 base pair (bp) 5′ *Bam*HI/*Pst*I fragment and a 900 bp 3′ *Hin*dIII/*Sal*I fragment were amplified from genomic AX2 wild-type DNA by PCR. The oligonucleotide primers used for the 5′ fragment were 5′-CGCGGGATCCGCATGTCTTTTGATTTAGAGAGTAATAGT-3′ and 5′-GCGCTGCAGAGAAAACTTATTAGTACTGATTGAAAA-3′, and the primers for the 3′ fragment were 5′-GCGAAGCTTGCTGAATATTTAACAACTTGTATGTCA-3′ and 5′-CGCGTCGACTTTATTTTTTTAATTGGCCTGATGGTTTTAA-3′. Both fragments were gel-purified after cleavage with *Bam*HI/*Pst*I and *Hin*dIII/*Sal*I, and cloned into the corresponding sites of pLPBLP that contains the blasticidin S resistance cassette[31]. The resulting vector was cleaved with *Bam*HI and *Sal*I and used to disrupt the *drf2* gene in wild-type cells.

Protein expression and purification. For the expression of various dDia2 constructs, the corresponding DNA fragments were amplified by PCR and cloned into the *Bam*HI and *Sal*I sites of pGEX-5x-1 (Amersham Pharmacia Biotech,

Piscataway, NJ). Expression and purification of GST, GST–Rac1A, GST–RacE, GST–RacC and GST–dDia2 constructs, and the subsequent GST-fusion protein binding assays with *D. discoideum* lysates were performed as described previously[24,30]. Full-length CapG was amplified from mouse cDNA as a *Bam*HI/*Hin*dIII fragment and cloned into these sites of vector pQE32. For uncapping experiments, recombinant *D. discoideum* capping protein Cap32/34 was also used[32]. Full-length Cap34 was amplified from cDNA as a *Sph*I/*Sal*I fragment and cloned into vector pQE30. Similarly, Cap32 was amplified as a *Sal*I/*Hin*dIII fragment and cloned downstream of Cap34. The Cap32 fragment carried an additional Shine–Dalgarno sequence at its 5′ end to allow for expression from a bicistronic operon in *E. coli*. His-tagged proteins were purified by standard procedures using Ni-NTA resin (Qiagen, Valencia, CA).

Antibodies, immunoprecipitation and western blotting. Polyclonal antibodies raised against dDia2 were obtained by immunizing female white New Zealand rabbits with recombinant GST-tagged FH2 (residues 624–1087) following standard procedures, then were affinity purified using purified GST–FH2 that was covalently coupled to cyanogen-bromide-activated agarose (Sigma, St Louis, MO). Immunolabelling and immunoprecipitations were performed with anti-dDia2 and anti-GFP polyclonal antibodies as described[23]. Immunoblotting was performed by standard procedures using dDia2-specific polyclonal antibodies, DGAP1-specific monoclonal antibody 216-394-1 (ref. 33) and GFP-specific monoclonal antibody 264-449-2 (ref. 34). Primary antibodies were visualized with phosphatase-coupled anti-mouse or anti-rabbit IgG (Dianova, Hamburg, Germany). Bound antibodies were quantified by densitometry using ImageJ software.

Yeast two-hybrid assay. Yeast two-hybrid interactions were analysed with the Matchmaker two-hybrid system 3 according to the manufacturer's instructions (Clontech/BD Biosciences, Palo Alto, CA). The activation domain of pGADT7 was fused to dDia2-FH1. Profilin I, II and III were expressed as full-length fusions with the Gal4-binding domain in plasmid pGBKT7.

Confocal microscopy and RICM. Microscopy was performed essentially as described[34]. For immunofluorescence, primary antibodies were visualized with Alexa-488-conjugated anti-rabbit IgG (Molecular Probes, Eugene, OR). F-actin was labelled with TRITC-conjugated phalloidin (Sigma). The specimens were analysed by confocal scanning microscopy using a LSM 510 Meta (Zeiss, Jena, Germany). The topography of the ventral cell surface, including filopodia and cell-to-substratum contacts, was imaged by RICM using the LSM 510 microscope and the 633-nm line of the He-Ne laser.

Quantification of cell motility. Analysis of cell motility of growth-phase cells was based on customized macros and plugins for ImageJ software (http://rsb.info.nih.gov/ij/). Random motility on glass coverslips in nutrient medium was determined by automatic centroid tracking after manual selection of the cells. Beforehand, images from time-lapse series were processed using a threshold binarization. Averaged velocities were calculated from 100 cell displacements during 30-s time intervals at ×20 magnification using an Axiovert 200 microscope (Zeiss). For each experiment a field containing approximately 20 cells was monitored.

Miscellaneous. Actin polymerization was measured by fluorescence spectroscopy with pyrene-labelled actin as described[35]. Actin polymerization experiments were performed in a buffer containing 10 mM imidazole, 2 mM $MgCl_2$, 0.2 mM $CaCl_2$, 1 mM Na-ATP and 50 mM KCl, pH 7.2. For the generation of F-actin seeds, G-actin was polymerized for 1 h at room temperature and subsequently vortexed vigorously for 1 min to mechanically shear the filaments. Routinely we used 0.1 nM actin as seeds per assay.

BIND identifiers. Four BIND identifiers (www.bind.ca) are associated with this manuscript: 295440, 295441, 295442 and 295443.

Note: Supplementary Information is available on the Nature Cell Biology website.

ACKNOWLEDGEMENTS

We thank J. Segall for discussions and for reading the manuscript, W. Witke for *CapG* cDNA and D. Rieger and M. Borath for excellent technical assistance. This work was supported by a grant to M.S. from the Deutsche Forschungsgemeinschaft and a grant to J.F. from the Friedrich-Baur-Stiftung.

COMPETING FINANCIAL INTERESTS

The authors declare that they have no competing financial interests.

Received 16 March 2005; accepted 29 April 2005
Published online at http://www.nature.com/naturecellbiology.

1. Evangelista, M., Zigmond, S. & Boone, C. Formins: signaling effectors for assembly and polarization of actin filaments. *J. Cell Sci.* **116,** 2603–2611 (2003).
2. Wallar, B. J. & Alberts, A. S. The formins: active scaffolds that remodel the cytoskeleton. *Trends Cell Biol.* **13,** 435–446 (2003).
3. Zigmond, S. H. Formin-induced nucleation of actin filaments. *Curr. Opin. Cell Biol.* **16,** 99–105 (2004).
4. Petersen, J., Nielsen, O., Egel, R. & Hagan, I. M. FH3, a domain found in formins, targets the fission yeast formin Fus1 to the projection tip during conjugation. *J. Cell Biol.* **141,** 1217–1228 (1998).
5. Alberts, A. S. Identification of a carboxyl-terminal diaphanous-related formin homology protein autoregulatory domain. *J. Biol. Chem.* **276,** 2824–2830 (2001).
6. Shimada, A. *et al.* The core FH2 domain of diaphanous-related formins is an elongated actin binding protein that inhibits polymerization. *Mol. Cell* **13,** 511–522 (2004).
7. Xu, Y. *et al.* Crystal structures of a formin homology-2 domain reveal a tethered dimer architecture. *Cell* **116,** 711–723 (2004).
8. Evangelista, *et al.* Bni1p, a yeast formin linking cdc42p and the actin cytoskeleton during polarized morphogenesis. *Science* **276,** 118–122 (1997).
9. Watanabe, N. *et al.* p140mDia, a mammalian homolog of *Drosophila* diaphanous, is a target protein for Rho small GTPase and is a ligand for profilin. *EMBO J.* **16,** 3044–3056 (1997).
10. Chan, D. C., Bedford, M. T. & Leder, P. Formin binding proteins bear WWP/WW domains that bind proline-rich peptides and functionally resemble SH3 domains. *EMBO J.* **15,** 1045–1054 (1996).
11. Sagot, I., Rodal, A. A., Moseley, J., Goode, B. L. & Pellman, D. An actin nucleation mechanism mediated by Bni1 and profilin. *Nature Cell Biol.* **4,** 626–631 (2002).
12. Kovar, D. R., Kuhn, J. R., Tichy, A. L. & Pollard, T. D. The fission yeast cytokinesis formin Cdc12p is a barbed end actin filament capping protein gated by profilin. *J. Cell Biol.* **161,** 875–887 (2003).
13. Evangelista, M., Pruyne, D., Amberg, D. C., Boone, C. & Bretscher, A. Formins direct Arp2/3-independent actin filament assembly to polarize cell growth in yeast. *Nature Cell Biol.* **4,** 32–41 (2002).
14. Peng, J., Wallar, B. J., Flanders, A., Swiatek, P. J. & Alberts, A. S. Disruption of the Diaphanous-related formin *Drf1* gene encoding mDia1 reveals a role for Drf3 as an effector for Cdc42. *Curr. Biol.* **13,** 534–545 (2003).
15. Pellegrin, S. & Mellor, H. The Rho family GTPase Rif induces filopodia through mDia2. *Curr. Biol.* **15,** 129–133 (2005).
16. Dai, J. & Sheetz, M. P. Membrane tether formation from blebbing cells. *Biophys. J.* **77,** 3363–3370 (1999).
17. Romero, S. *et al.* Formin is a processive motor that requires profilin to accelerate actin assembly and associated ATP hydrolysis. *Cell* **119,** 419–429 (2004).
18. Kovar, D. R. & Pollard, T. D. Insertional assembly of actin filament barbed ends in association with formins produces piconewton forces. *Proc. Natl Acad. Sci. USA* **101,** 14725–14730 (2004).
19. Eichinger, L. *et al.* The genome of the social amoeba *Dictyostelium discoideum*. *Nature* **435,** 43–57 (2005).
20. Kitayama, C. & Uyeda, T. Q. ForC, a novel type of formin family protein lacking an FH1 domain, is involved in multicellular development in *Dictyostelium discoideum*. *J. Cell Sci.* **116,** 711–723 (2003).
21. Haugwitz, M., Noegel, A. A., Karakesisoglou, J. & Schleicher, M. *Dictyostelium* amoebae that lack G-actin-sequestering profilins show defects in F-actin content, cytokinesis, and development. *Cell* **79,** 303–314 (1994).
22. Rivero, F., Dislich, H., Glöckner, G. & Noegel, A. A. The *Dictyostelium discoideum* family of Rho-related proteins. *Nucleic Acids Res.* **29,** 1068–1079 (2001).
23. Faix, J. *et al.* Recruitment of cortexillin into the cleavage furrow is controlled by Rac1 and IQGAP-related proteins. *EMBO J.* **20,** 3705–3715 (2001).
24. Dumontier, M., Höcht, P., Mintert, U. & Faix, J. Rac1 GTPases control filopodia formation, cell motility, endocytosis, cytokinesis and development in *Dictyostelium*. *J. Cell Sci.* **113,** 2253–2265 (2000).
25. Small, J. V., Stradal, T., Vignal, E. & Rottner, K. The lamellipodium: where motility begins. *Trends Cell Biol.* **12,** 112–120 (2002).
26. Han, Y. H. *et al.* Requirement of a vasodilator-stimulated phosphoprotein family member for cell adhesion, the formation of filopodia, and chemotaxis in *Dictyostelium*. *J. Biol. Chem.* **277,** 49877–49887 (2002).
27. Svitkina, T. M. *et al.* Mechanism of filopodia initiation by reorganization of a dendritic network. *J. Cell Biol.* **160,** 409–421 (2003).
28. Lebrand, C. *et al.* Critical role of Ena/VASP proteins for filopodia formation in neurons and in function downstream of Netrin-1. *Neuron* **42,** 37–49 (2004).
29. Hug, C. *et al.* Capping protein levels influence actin assembly and cell motility in *Dictyostelium*. *Cell* **81,** 591–600 (1995).
30. Faix, J. *et al.* The IQGAP-related protein DGAP1 interacts with Rac and is involved in the modulation of the F-actin cytoskeleton and control of cell motility. *J. Cell Sci.* **111,** 3059–3071 (1998).
31. Sutoh, K. A transformation vector for *Dictyostelium discoideum* with a new selectable marker bsr. *Plasmid* **2,** 150–154 (1993).
32. Hartmann, H., Noegel, A. A., Eckerskorn, C., Rapp, S. & Schleicher, M. Ca^{2+}-independent F-actin capping proteins. *J. Biol. Chem.* **264,** 12639–12647 (1989).
33. Faix, J. & Dittrich, W. DGAP1, a homologue of rasGTPase activating proteins that controls growth, cytokinesis, and development in *Dictyostelium discoideum*. *FEBS Lett.* **394,** 251–257 (1996).
34. Weber, I. *et al.* Cytokinesis mediated through the recruitment of cortexillins into the cleavage furrow. *EMBO J.* **18,** 586–594 (1999).
35. Eichinger, L. & Schleicher, M. Characterization of actin- and lipid-binding domains in severin, a Ca^{2+}-dependent F-actin fragmenting protein. *Biochemistry* **31,** 4779–4787 (1992).

nature cell biology

Movie 1: Confocal time lapse series of a GFP-dDia2 cell.

Movie 2: 3D reconstruction of a GFP-dDia2 cell double labeled for F-actin (red) and dDia2 (green).

Movie 3: RICM time lapse series of a wild-type cell.

Movie 4: RICM time lapse series of a dDia2-null cell.

Movie 5: RICM time lapse series of a GFP-dDia2 cell.